ω-Imidazolyl- and ω-Tetrazolylalkylcarbamates as Inhibitors of Fatty Acid Amide Hydrolase: Biological Activity and in vitro Metabolic Stability

Tobias Terwege,[a] Walburga Hanekamp,[a] David Garzinsky,[a] Simone König,[b] Oliver Koch,[c] and Matthias Lehr*[a]

Fatty acid amide hydrolase (FAAH) is a serine hydrolase that terminates the analgesic and anti-inflammatory effects of endocannabinoids such as anandamide. Herein, structure–activity relationship studies on a new series of aryl N-(ω-imidazolyl- and ω-tetrazolylalkyl)carbamate inhibitors of FAAH were investigated. As one result, a pronounced increase in inhibitory potency was observed if a phenyl residue attached to the carbamate oxygen atom was replaced by a pyridin-3-yl moiety. The most active compounds exhibited IC$_{50}$ values in the low nanomolar range. In addition, investigations on the metabolic properties of these inhibitors were performed. In rat liver homogenate and in porcine plasma, the extent of their degradation was shown to be strongly dependent on the kind of aryl residue bound to the carbamate as well as on the length and type of the alkyl spacer connecting the carbamate group with the heterocyclic system. With the aid of esterase inhibitors it was shown that in porcine plasma, carboxylesterase-like enzymes and paraoxonase are involved in carbamate cleavage. Moreover, it was found that highly active pyridin-3-yl carbamates reacted with albumin, which led to covalent albumin adducts.

Introduction

N-Arachidonoylethanolamine—more commonly known as anandamide—is one principal endocannabinoid in the mammalian organism.[1,2] It is formed "on demand" during several physiological and pathological processes, for which it appears to exert analgesic and anti-inflammatory effects through activation of the cannabinoid receptors CB$_1$ and CB$_2$.[3–5]

An important enzyme in the endocannabinoid metabolism is the membrane-bound fatty acid amide hydrolase (FAAH). FAAH, which belongs to the serine-hydrolase family, is responsible for the rapid degradation of the lipid mediator anandamide into arachidonic acid and ethanolamine.[6–9] Inhibition of FAAH is thought to elevate anandamide levels and prolong its activity. Therefore, inhibitors of this enzyme may represent new agents against pain and inflammation. In the past years, many potent inhibitors of FAAH have been discovered.[10–14] The majority of these compounds are substances that form covalent bonds with the catalytic serine residue of the active site of FAAH such as carbamates 1 (URB 597)[15] and 2,[16] activated ketone derivatives such as α-keto heterocycle 3[17] and propan-2-one 4,[18] and urea derivatives such as 5 (PF-04457845) (Figure 1).[19] The latter compound is actually being examined

in clinical trials for cannabis withdrawal,[20a] fear response,[20b] and activity in Tourette syndrome.[20c]

In a recent study, we used imidazolylalkylcarbamate derivative 2 as a lead structure for inhibitor development.[21] Because we became familiar with the preparation of arylated pyrroles during development of cyclooxygenase and 5-lipoxygenase inhibitors,[22] we synthesized substances in which the diphenyli-

[a] Dr. T. Terwege, W. Hanekamp, D. Garzinsky, Prof. Dr. M. Lehr
Institute of Pharmaceutical and Medicinal Chemistry
University of Münster, Corrensstrasse 48, 48149 Münster (Germany)
E-mail: lehrm@uni-muenster.de

[b] Prof. Dr. S. König
Core Unit Proteomics, Interdisciplinary Center for Clinical Research (IZKF)
University of Münster, Röntgenstrasse 21, 48149 Münster (Germany)

[c] Dr. O. Koch
Faculty of Chemistry and Chemical Biology
TU Dortmund University, Otto-Hahn-Strasse 6, 44227 Dortmund (Germany)
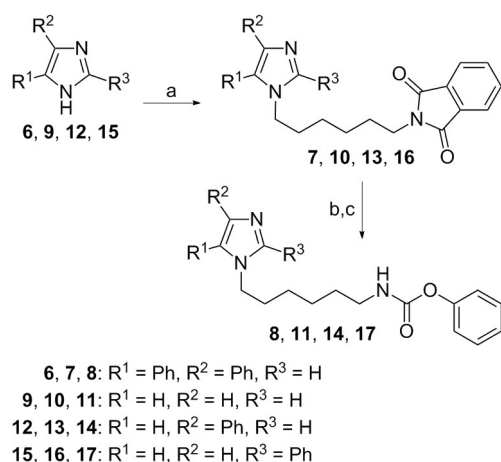
Figure 1. Structures of known FAAH inhibitors.

midazole heterocycle was replaced by a pyrrole scaffold. During structure–activity relationship studies, it became evident that pyrrole derivatives bearing only one phenyl ring at the 2-position of the heterocycle were significantly more active against FAAH than the corresponding 2,3-diphenylpyrrole derivatives. The starting point of the present study was the question as to whether the same effects could be found for diphenylimidazole **2**. The designed phenyl imidazolylalkylcarbamates should be systematically varied to increase their potency and to obtain new insight into the relationship between the structure of this substance class and FAAH inhibition. Furthermore, we focused our attention on the stability of the carbamate target compounds in aqueous solution and in biological environments, namely, liver homogenate and blood plasma, because carbamate moieties are known to be susceptible to hydrolytic cleavage.

Results and Discussion

Chemistry

Compound **8**, which is a derivative of lead compound **2**, lacks the methyl substituent at the 2-position of the imidazole ring; it was prepared in three steps from 4,5-diphenylimidazole (**6**) (Scheme 1). Briefly, alkylation of the imidazole nitrogen atom

6, 7, 8: R^1 = Ph, R^2 = Ph, R^3 = H
9, 10, 11: R^1 = H, R^2 = H, R^3 = H
12, 13, 14: R^1 = H, R^2 = Ph, R^3 = H
15, 16, 17: R^1 = H, R^2 = H, R^3 = Ph

Scheme 1. *Reagents and conditions*: a) *N*-(6-Bromohexyl)phthalimide, K$_2$CO$_3$, DMSO, 50–70 °C, 1–5 h; b) hydrazine hydrate, EtOH, reflux, 2–3 h; c) phenyl chloroformate, Et$_3$N, THF, RT, 2 h (for **8**) or phenyl chloroformate, ethyl(diisopropyl)amine, THF, RT, 4 h (for **11**) or phenyl chloroformate, Et$_3$N, CH$_2$Cl$_2$, 0 °C to RT, 1–4 h (for **14** and **17**).

with *N*-(6-bromohexyl)phthalimide under basic conditions afforded intermediate **7**. Subsequent cleavage of the phthalimide protecting group with hydrazine provided the free amine, which was immediately treated with phenyl chloroformate to yield target compound **8**. A derivative of **8**, that is, compound **11**, in which the imidazole phenyl substituents were replaced by hydrogen atoms, and corresponding 2-phenyl- and 4-phenylimidazoles **14** and **17** were synthesized by the same route starting from imidazole (**9**) and phenylimidazoles **12** and **15**, respectively.

Because alkylation of 4-phenylimidazole (**12**) with *N*-(6-bromohexyl)phthalimide entirely occurred at the nitrogen atom in the 1-position and not, which might be possible in principle, at the nitrogen atom in the 3-position, the desired 5-phenyl-substituted imidazole could not be afforded as a side product of this reaction. Therefore, for the preparation of the target substance with a 5-phenylimidazole residue, an alternative synthetic approach was developed (Scheme 2). Analogously to a published procedure,[23] imidazole intermediate **9** was arylated at C5 by Pd-catalyzed coupling with bromobenzene. Treatment of obtained 5-phenyl-substituted imidazole derivative **18** with hydrazine and subsequent reaction of the liberated amino group with phenyl chloroformate led to target compound **19**.
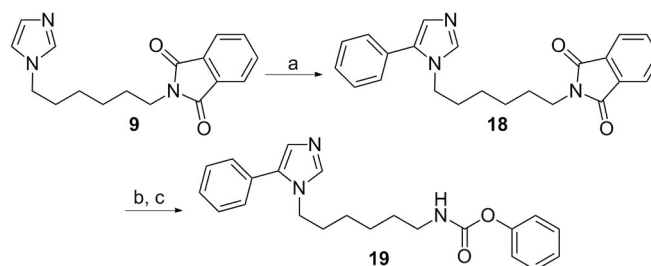
Scheme 2. *Reagents and conditions*: a) Bromobenzene, tri(2-furyl)phosphine, Pd(OAc)$_2$, K$_2$CO$_3$, DMF, 140 °C, 16 h; b) hydrazine hydrate, EtOH, reflux, 3 h; c) phenyl chloroformate, ethyl(diisopropyl)amine, THF, RT, 4 h.

Derivatives of 2-phenylimidazole **17**, that is, compounds **20–24** possessing substituents on the phenyl ring and compounds **25–27** possessing alkyl spacers with various lengths, were prepared by following a procedure similar to that used to prepare **17** but with the appropriate starting materials.[24]

For the synthesis of hexylcarbamate **30** with the terminal 2-phenylimidazole moiety replaced by a 5-phenyltetrazole heterocycle, 5-phenyl-1*H*-tetrazole was first treated with *N*-(6-bromohexyl)phthalimide in acetonitrile or DMSO in the presence of K$_2$CO$_3$. In both cases, 5-phenyl-1*H*-tetrazole intermediate **29** was only obtained as a minor product, whereas 5-phenyl-2*H*-tetrazole **31** was isolated as the main product (Scheme 3). Transformation of the phthalimide residues of both isomers into phenylcarbamate groups was conducted in a manner similar to that described above to afford target compounds **30** and **32**. The structures of the isomers were determined by NOE experiments and ^{13}C NMR spectroscopy. Thus, the ^{13}C NMR signal of the C5 atom of the 5-phenyl-1*H*-tetrazole appears at significantly higher field ($\delta \approx 154$ ppm) than the corresponding signal of the 5-phenyl-2*H*-tetrazole ($\delta \approx 164$ ppm).[25,26]

The analogues of 5-phenyl-2*H*-tetrazole **32** with the tetrazole phenyl ring replaced by chlorophenyl, pyridinyl, or benzyl residues, that is, compounds **33–38** and **44**, were prepared in a manner analogous to that used to prepare **32** starting from the appropriately substituted tetrazoles. The synthesis of 4-carboxyphenyl-substituted 2*H*-tetrazole **43** started from 4-cyanobenzoic acid *tert*-butyl ester (Scheme 4). The nitrile group of
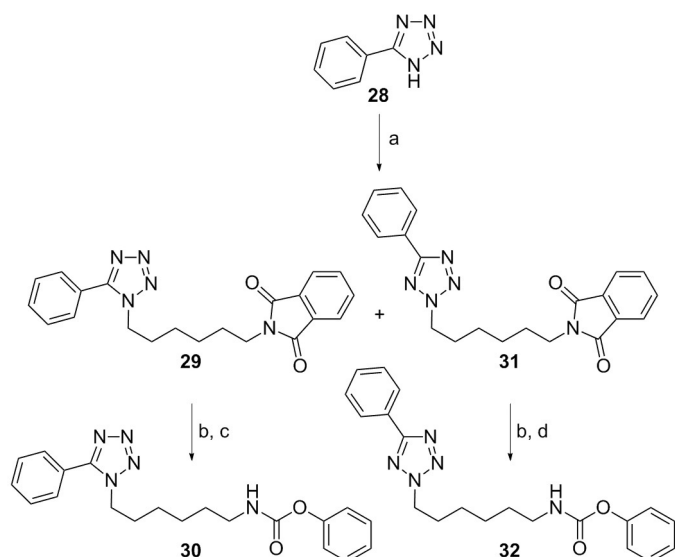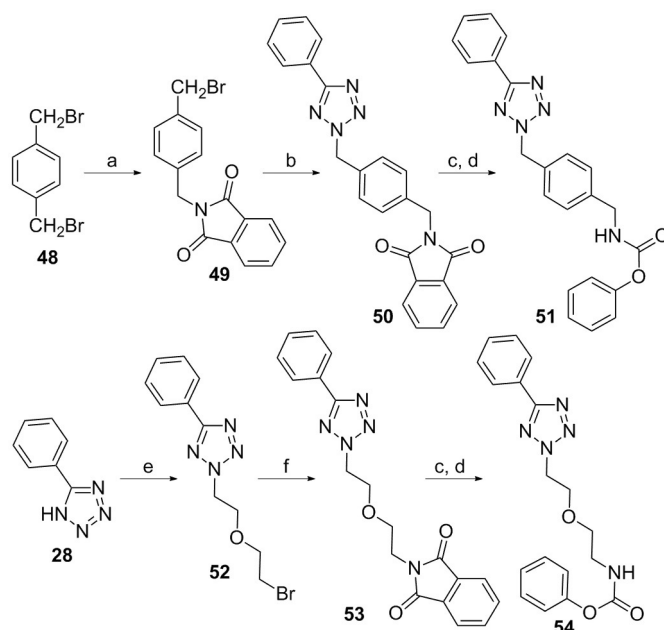
Scheme 3. *Reagents and conditions*: a) *N*-(6-Bromohexyl)phthalimide, K$_2$CO$_3$, KI, CH$_3$CN, reflux, 3 h or *N*-(6-bromohexyl)phthalimide, K$_2$CO$_3$, DMSO, 60–70 °C, 1 h; b) hydrazine hydrate, EtOH, reflux, 3 h; c) phenyl chloroformate, ethyl(diisopropyl)amine, THF, RT, 2 h; d) phenyl chloroformate, Et$_3$N, CH$_2$Cl$_2$, 0 °C to RT, 1 h.
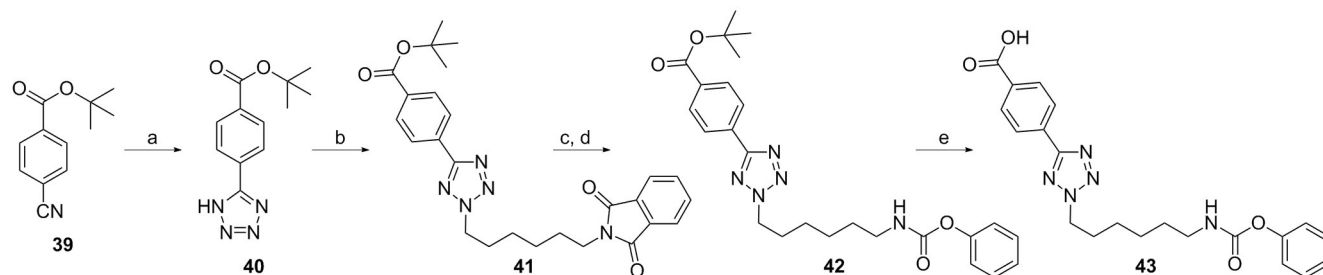
Scheme 5. *Reagents and conditions*: a) Potassium phthalimide, DMF, 80 °C, 4 h; b) 5-phenyl-1*H*-tetrazole, K$_2$CO$_3$, KI, CH$_3$CN, reflux, 3 h; c) hydrazine hydrate, EtOH, reflux, 2 h; d) phenyl chloroformate, ethyl(diisopropyl)amine, THF, RT, 2 h; e) bis(2-bromoethyl)ether, K$_2$CO$_3$, KI, CH$_3$CN, reflux, 3 h; f) potassium phthalimide, DMF, 130 °C, 2 h.

this compound was converted into a tetrazole (see compound **40**) by reaction with trimethylsilyl azide. Then, the phenyl *N*-alkylcarbamate residue was introduced in a manner similar to that described above. Finally, the *tert*-butyl ester group of intermediate **42** was cleaved with trifluoroacetic acid to afford target compound **43**.

The synthesis of derivatives of **32** with shorter and longer alkyl spacers, that is, compounds **45**–**47**, or with fluoro or methoxy substituents at the carbamate phenyl residue, that is, compounds **55**–**58**, was performed analogously by using the appropriate *N*-(6-bromoalkyl)phthalimide and substituted phenyl chloroformate, respectively.

The preparation of analogues of **32** with 1,4-phenylenebis(methylene) or ethoxyethyl residues connecting the tetrazole and the carbamate scaffolds (see compounds **51** and **54**) were prepared as outlined in Scheme 5 by using reactions similar to those already described.

Pyridin-3-yl carbamates **59** and **60** were synthesized by treatment of their amine precursors with pyridin-3-yl chlorofor-

mate (Scheme 6), which was obtained by treating 3-hydroxypyridine with trichloromethyl chloroformate in CH$_2$Cl$_2$ in the presence of ethyl(diisopropyl)amine.

Inhibition of FAAH

The carbamate derivatives prepared in this study were tested for their ability to inhibit FAAH from rat brain by monitoring cleavage of a fluorogenic substrate by HPLC fluorescence detection as previously described.[27,28]

To investigate the impact of the methyl residues and the two phenyl residues at the imidazole scaffold on the inhibitory potency of lead **2**, we synthesized derivatives lacking one or more of these substituents. Replacement of the imidazole methyl substituent by a hydrogen atom (i.e., compound **8**) did not affect FAAH inhibition (Table 1). However, the inhibitory potency decreased approximately 12-fold upon removing the
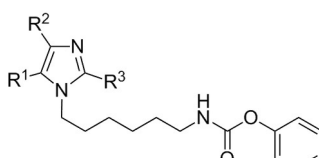
Scheme 4. *Reagents and conditions*: a) Trimethylsilyl azide, tetrabutylammonium fluoride hydrate, 120 °C, 3 h; b) *N*-(6-bromohexyl)phthalimide, K$_2$CO$_3$, KI, CH$_3$CN, reflux, 3 h; c) hydrazine hydrate, EtOH, reflux, 3 h; d) phenyl chloroformate, ethyl(diisopropyl)amine, THF, RT, 2 h; e) TFA, CH$_2$Cl$_2$, RT, 24 h.
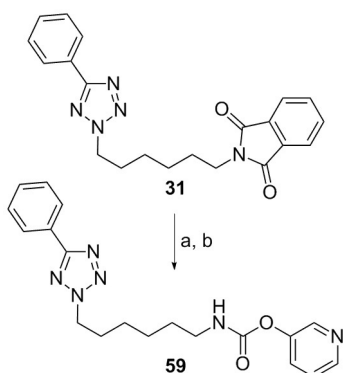
Scheme 6. *Reagents and conditions*: a) Hydrazine hydrate, EtOH, reflux, 2 h; b) pyridin-3-yl chloroformate, ethyl(diisopropyl)amine, THF, RT, 2 h.

Table 1. Effect of varying imidazole scaffold substituents on the inhibition of FAAH.

Compd	R^1	R^2	R^3	IC$_{50}$ [μM][a]
8	Ph	Ph	H	0.49
11	H	H	H	6.0
19	Ph	H	H	0.48
14	H	Ph	H	0.88
17	H	H	Ph	0.29
20	H	H	4-ClC$_6$H$_4$	0.42
21	H	H	3-ClC$_6$H$_4$	0.054
22	H	H	3-FC$_6$H$_4$	0.11
23	H	H	3-MeC$_6$H$_4$	0.075
24	H	H	3-MeOC$_6$H$_4$	0.29
2 (BMS-1)	Ph	Ph	Me	0.47
1 (URB 597)				0.10

[a] Values are the means of at least two independent determinations; errors are within $\pm$20%.

two phenyl residues (i.e., compound **11**). Looking at the IC$_{50}$ values of the imidazole derivatives with only one phenyl substituent in the 4- or 5-position of the imidazole (i.e., compound **19** or **14**) it became evident that it was not necessary for both residues to be present simultaneously. The compound with a phenyl residue in the neighborhood of the *N*-alkyl chain (i.e., compound **19**) was equipotent to diphenylimidazole **8**, and the derivative with the phenyl ring and the alkyl chain in the 1,3-positions (i.e., compound **14**) was still half as active. The activity increased nearly twofold by moving the phenyl residue of **19** to the other side of the imidazole ring between the two nitrogen atoms. The IC$_{50}$ value of obtained compound **17** was 0.29 μM.
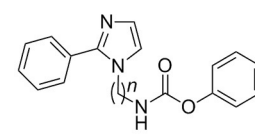
Next, we examined the effects of substituents on the imidazole phenyl residue of **17**. Whereas compound **20** possessing a chlorine atom in the *para* position showed reduced activity against FAAH, *meta*-chloro derivative **21** (IC$_{50}$: 0.053 μM)

showed an inhibitory potency that was approximately fivefold higher than that of **17** (Table 1). Fluoro and methyl substituents at this *meta* position (i.e., compounds **22** and **23**) led to an increase in activity that was less pronounced, whereas a methoxy group (i.e., compound **24**) did not show any effect.

To evaluate the role of the alkyl chain of **17** on FAAH inhibition, we varied the length of this structural element. Elongation by one carbon atom to give compound **26** did not affect the enzyme inhibition remarkably, whereas elongation by two carbon atoms and abbreviation by one carbon atom to give compounds **25** and **27**, respectively, slightly decreased the potency (Table 2).
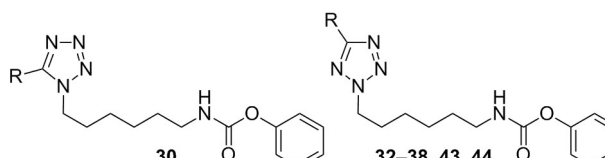
Additionally, we wanted to study the effect of replacing the two unsubstituted carbon atoms in the imidazole ring of **17** by nitrogen atoms. As shown in Table 3, this structural variation led to a decrease in FAAH inhibition. 5-Phenyl-1*H*-tetrazole **30** was approximately fourfold less active than analogous phenylimidazole **17**. During the synthesis of an intermediate of tetrazole **30**, an isomeric 5-phenyl-2*H*-tetrazole derivative was obtained and it was further treated to test compound **32**. Inter-

Table 2. Effect of varying the length of the alkyl chain on the inhibition of FAAH.

Compd	n	IC$_{50}$ [μM][a]
25	5	0.43
17	6	0.29
26	7	0.24
27	8	0.40

[a] Values are the means of at least two independent determinations; errors are within $\pm$20%.

Table 3. Effect of a tetrazole moiety on the inhibition of FAAH.

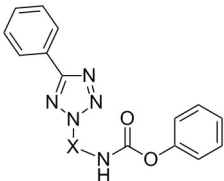| Compd	R	IC$_{50}$ [μM][a]
30	Ph	1.3
32	Ph	0.60
33	4-ClC$_6$H$_4$	0.57
34	3-ClC$_6$H$_4$	0.18
35	2-ClC$_6$H$_4$	0.20
36	Pyridin-4-yl	1.2
37	Pyridin-3-yl	0.70
38	Pyridin-2-yl	0.28
43	4-HCO$_2$C$_6$H$_4$	> 10 (23% at 10 μM)
44	Bn[b]	0.25

[a] Values are the means of at least two independent determinations; errors are within $\pm$20%. [b] Bn = benzyl.

estingly, the inhibitory potency of this derivative was twice as high as that of 5-phenyl-1*H*-tetrazole **30**. Thus, in contrast to the phenylimidazoles, shifting the phenyl residue from the α position to the β position of the alkylated nitrogen atom of the tetrazole had a positive effect on activity.

To further the study of the structure–activity relationship, 5-phenyl-2*H*-tetrazole **32** was used as a lead compound. First, the phenyl ring attached to the tetrazole scaffold was replaced by chlorophenyl, pyridyl, carboxyphenyl, and benzyl residues (Table 3). Whereas a lipophilic chlorine atom in the 4-position of the phenyl moiety (i.e., compound **33**) did not affect FAAH inhibition, a chlorine atom in the 3- or 2-position (i.e., compound **34** or **35**) increased the potency threefold. Exchange of the phenyl ring by an electron-withdrawing pyridyl moiety resulted in different effects in dependence of the position of the pyridine nitrogen atom. Pyridin-4-yl derivative **36** was only half as active as phenyl-substituted lead **32**. In contrast, pyridin-3-yl derivative **37** maintained the activity, whereas pyridin-2-yl derivative **38** showed FAAH inhibition that increased twofold. A polar carboxy group in the *para* position of the phenyl residue was not tolerated; the IC$_{50}$ value of corresponding tetrazole **43** rose to a value above 10 μm. On the other hand, the activity of derivative **44** with a more flexible benzyl residue was twofold higher than that of phenyl-substituted compound **32**.

Next, we examined the relationship between the length of the alkyl spacer and the inhibitory activity of the compounds (Table 4). The highest potencies were observed for the 5-

Table 4. Effect of varying the length of the alkyl spacer on the inhibition of FAAH.

Compd	X	IC$_{50}$ [μm][a]
45	(CH$_2$)$_5$	0.49
32	(CH$_2$)$_6$	0.60
46	(CH$_2$)$_7$	0.081
47	(CH$_2$)$_8$	0.11
51	4-CH$_2$C$_6$H$_4$CH$_2$	0.26
54	(CH$_2$)$_2$O(CH$_2$)$_2$	5.2
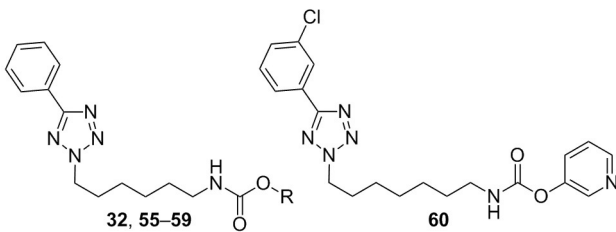
[a] Values are the means of at least two independent determinations; errors are within ±20%.

phenyl-2*H*-tetrazole derivatives with C$_7$ and C$_8$ alkyl chains, that is, for compounds **46** and **47**. Remarkably, in the case of the corresponding 2-phenylimidazoles, the optimal chain length was six to seven carbon atoms (Table 2). With IC$_{50}$ values of ~0.1 μm, the most active tetrazoles of this series, that is, compounds **46** and **47**, were approximately twofold more potent than their imidazole counterparts, namely, compounds **17** and **26**.

Replacing the central carbon atom of the pentyl chain of **45** by a polar oxygen atom to give **54** resulted in an approximate 10-fold decrease in activity. In contrast, rigidization of the alkyl spacer of **32** by incorporating it into a phenyl ring system to give **51** was well tolerated by the enzyme (Table 4).

Sit et al.[16] found that the activity of their phenyl *N*-imidazolylalkylcarbamates could be enhanced approximately twofold if the *ortho* position of the phenyl ring of the carbamate moiety was substituted with a fluorine atom. The same effect was observed after introduction of a fluorine atom at the corresponding position of *N*-tetrazoylalkylcarbamate **32** to yield compound **56** (Table 5). A fluorine atom or a more polar methoxy

Table 5. Effect of fluorine and polar groups in the carbamate moiety on the inhibition of FAAH.

Compd	R	IC$_{50}$ [μm][a]
32	Ph	0.60
55	4-FC$_6$H$_4$	0.66
56	2-FC$_6$H$_4$	0.33
57	4-MeOC$_6$H$_4$	0.65
58	2-MeOC$_6$H$_4$	> 10
59	Pyridin-3-yl	0.011
60		0.0053

[a] Values are the means of at least two independent determinations; errors are within ±20%.

group in the *para* position of the carbamate phenyl residue to give **55** or **57** did not enhance the FAAH inhibition, whereas a methoxy group in the *ortho* position of compound **58** led to a sharp drop in activity.

In the literature, a series of very potent pyridin-3-yl carbamate inhibitors of FAAH is described.[29] For this reason, we recently synthesized *N*-indolylalkylcarbamates with such a structural element.[21] By this way, highly active compounds with IC$_{50}$ values in the low nanomolar range were obtained. In the present study, replacement of the phenyl residue of carbamate **32** by a pyridin-3-yl substituent also resulted in a drastic increase in activity (Table 5). Synthesized pyridin-3-yl derivative **59** (IC$_{50}$: 0.011 μm) was approximately 60-fold more active than phenyl-substituted analogue **32** (IC$_{50}$: 0.60 μm).

Taken together, we found that introduction of a chlorine atom in the *meta* position of tetrazole phenyl residue to give **34**, elongation of the hexyl spacer by one carbon atom to give **46**, and replacement of the phenyl carbamate moiety by a pyridin-3-yl carbamate to give **59** caused a significant increase in FAAH inhibitory potency. Therefore, we combined these three structural elements in one molecule. The biological testing of resulting compound **60** showed that the observed effects

were not additive (Table 5). With an IC$_{50}$ value of 0.0053 µM, **60** was only twice as active as pyridin-3-yl carbamate **59**, although a chlorine atom increased the activity ninefold and an additional carbon atom in the alkyl chain increased the activity sevenfold in the case of corresponding phenyl carbamate **32**.

Known carbamate inhibitors of FAAH inhibit the enzyme by covalent carbamoylation of the active site serine.[30] To investigate whether our new carbamate compounds also affected the enzyme in such a manner, the reversibility of enzyme inhibition by phenyl carbamate **46** and pyridin-3-yl carbamate **59** was studied following a published procedure.[31] The enzyme preparation was pre-incubated with these inhibitors at concentrations ranging from approximately 0.1- to 10-fold their IC$_{50}$ value. After 60 min, rapid 10-fold dilution with a solution of the substrate in phosphate-buffered saline (PBS) containing 0.2% Triton X-100 was performed and incubation was continued for an additional 60 min before measuring the IC$_{50}$ values of the inhibitors against FAAH as per usual. By this procedure, the IC$_{50}$ values of both compounds significantly declined from 63 nM for **46** and 8 nM for **59** (without pre-incubation) to less than 1 nM (with 60 min pre-incubation). More specifically, **46** and **59** inhibited FAAH activity at 1 nM by (78±5) and (81±7)% (mean±SD, $n=3$), respectively. (Note: IC$_{50}$ values determined for **46** and **59** in the control incubations without pre-incubation in these experiments were slightly lower than those listed in Tables 4–6. These deviations result from exchange of the Tris buffer used in the FAAH assay first by PBS; see the Experimental Section below, *Inhibition of FAAH*, for additional information). By not starting the enzyme reaction immediately after 10-fold dilution of the enzyme preparation but 60 min later by the addition of a small volume of a concentrated substrate solution in DMSO to the enzyme preparation diluted with Triton X-100 in PBS, the inhibition values did not change significantly. The IC$_{50}$ values were still below 1 nM [(65±4)% for **46** and (73±7)% for **59** inhibition at 1 nM, mean±SD, $n=3$], Thus, there is strong evidence that the inhibitors interact with the enzyme in a long-lasting covalent and irreversible manner and not in a rapid or slow mode of reversible inhibition.

Molecular docking

We also performed docking experiments to obtain more precise insight into the structure–activity relationships of the synthesized compounds. These studies based on the crystal structure of FAAH in complex with α-keto heterocycle inhibitor **3** (PDB ID: 3K7F; for the structure of **3**, see Figure 1).[17] X-ray analysis of this complex revealed that **3** is covalently bound to the catalytic Ser241 residue through its electrophilic carbonyl group (Figure 2).

Our carbamate inhibitors were docked in the tetrahedral transition state form emerging during a covalent reaction with the active site serine. Figure 3a shows exemplarily the two main conformations of phenyl and pyridin-3-yl *N*-arylhexylcarbamates **32** and **59** that can be seen throughout most of the compounds with a C$_6$ alkane linker: a kinked conformation showing overlap of the terminal phenyl residues of **32** and **59** with the terminal phenyl moiety of covalently bound inhibitor **3**, and a more extended conformation showing overlap of the tetrazole rings of **32** and **59** with the phenyl residue of **3**. Inter-

Table 6. Inhibitory potency against FAAH and stability in biological environments of selected ω-(phenyltetrazolyl)alkylcarbamates and the stability of putative metabolites of these compounds.

32, 34, 45–47, 51, 54, 59, 60   **61** X = (CH$_2$)$_6$ **62** X = (CH$_2$)$_5$
63 X = (CH$_2$)$_7$ **64** X = (CH$_2$)$_6$

Compd	X	R^1	R^2	IC$_{50}$ [µM][a]	Liver S9 [%][b]	Stability [%][c]	
						plasma	albumin
45	(CH$_2$)$_5$	H	Ph	0.49	59±2	54±11	100±1
32	(CH$_2$)$_6$	H	Ph	0.60	84±8	58±9	92±7
46	(CH$_2$)$_7$	H	Ph	0.081	86±3	21±5	93±8
47	(CH$_2$)$_8$	H	Ph	0.11	71±2	51±7	98±5
51	4-CH$_2$C$_6$H$_4$CH$_2$	H	Ph	0.26	85±6	44±4	90±10
54	(CH$_2$)$_2$O(CH$_2$)$_2$	H	Ph	5.2	50±5	94±5	91±7
34	(CH$_2$)$_6$	Cl	Ph	0.18	91±9	70±7	94±9
59	(CH$_2$)$_6$	H	Pyridin-3-yl	0.011	48±5	0	32±3
60	(CH$_2$)$_7$	Cl	Pyridin-3-yl	0.0053	37±5	0	20±7
61				–	37±2	0	95±5
62				–	0	76±6	97±3
63				–	41±3	0	93±7
64				–	0	76±6	86±4
1 (URB 597)				0.10	82±4	77±6	95±7

[a] Values are the means of at least two independent determinations; errors are within ±20. [b] Percent of parent remaining after incubation with rat liver S9 fractions for 30 min in the presence of the cofactor NADPH; values are means±SD of independent determinations ($n=3$). [c] Percent of parent remaining after incubation with porcine plasma or porcine albumin for 30 min; values are means±SD of independent determinations ($n=3$).
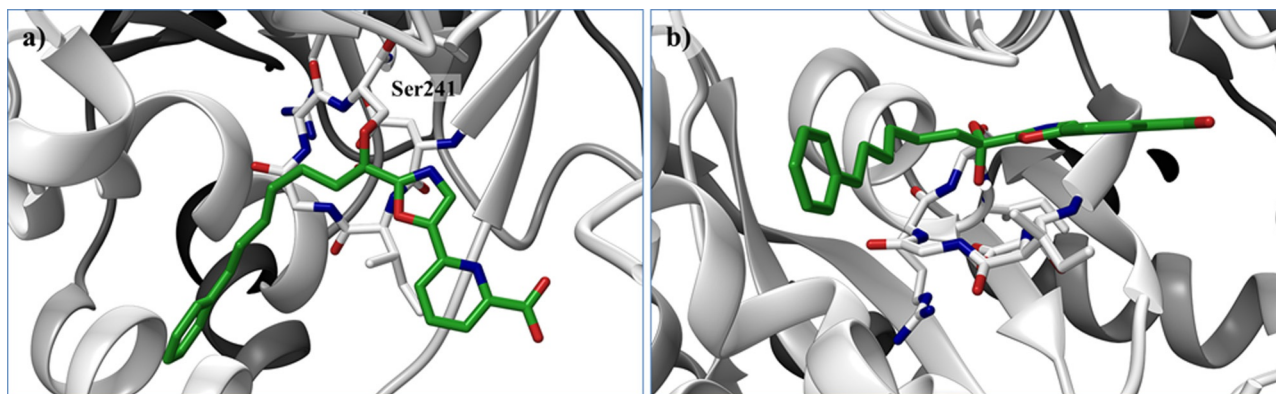
Figure 2. Compound **3** (green) covalently bound to FAAH according to PDB ID: 3K7F: a) View with focus on the covalent interaction of the inhibitor with Ser241; b) view that shows stabilizing interactions with the backbone amide groups of a loop.
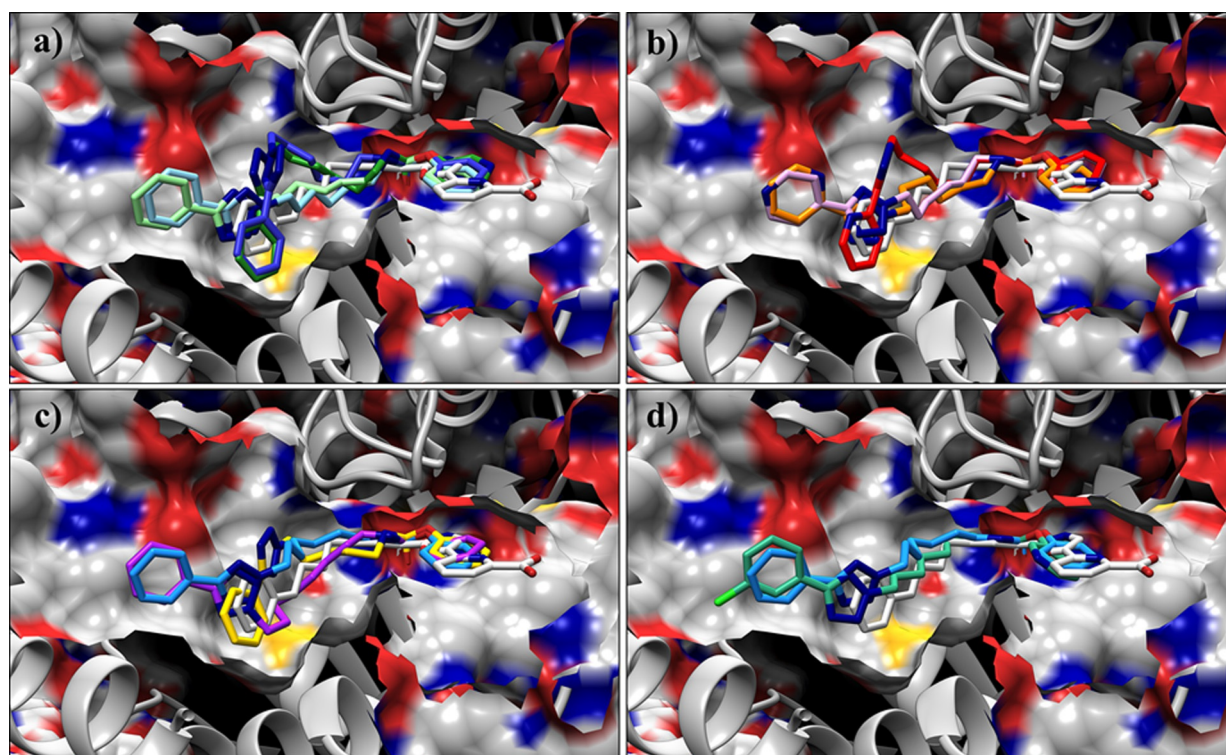
Figure 3. Docking poses of active carbamate inhibitors in comparison with the binding of covalent inhibitor **3** in its crystal structure with FAAH[17] (light gray): a) compound **32** and **59** in kinked conformation (dark green and dark blue) and in extended conformation (light green and light blue); b) compounds **36** (pink) and **38** (kinked: red, extended: orange); c) compounds **45** (yellow), **46** (light blue), and **47** (magenta); d) compounds **46** (light blue) and **60** (light green).

estingly, **32** and **59** show identical poses, although their activities are quite different (Table 5). This indicates a huge influence of the phenyl and pyridine moieties bound to the carbamate oxygen atom, either during entry of the molecules into the active site or with regard to their reactivity with the catalytic serine residue.

Figure 3b shows the extended docking poses of pyridyltetrazole derivatives **36** and **38** (Table 3) and the kinked pose of **38**, which is missing in the cases of compounds **36** and **37**. One can postulate that the positions of the pyridine nitrogen atom in pyridin-4-yltetrazole **36** and pyridin-3-yltetrazole **37**

are disfavored in the kinked conformation owing to the fact that the nitrogen atom would be within the hydrophobic pocket. In contrast, the pyridine nitrogen atom in pyridin-2-yltetrazole **38** points toward the solution in the kinked conformation.

Within the compound series of pentylcarbamate **45**, heptylcarbamate **46**, and octylcarbamate **47** (Figure 3c), compound **45** is the one to exhibit a kinked conformation. This can be explained by the shorter alkane linker that, presumably, does not allow an extended conformation. In contrast, the highly active heptyl- and octylcarbamates **46**, **47**, and **60** (Figure 3c,d) can

only be docked in an extended conformation: the alkane linker seems to be too long for a kinked conformation. In the docking poses of these three compounds, the tetrazole ring lies in a position similar to that of the terminal phenyl residue of inhibitor **3**, as shown by the crystal structure. In addition, the *meta*-chloro substituent of compound **60** fits into the hydrophobic pocket, which explains the favorable effects of such a substituent.

Owing to the hydrophobic character of the entry tunnel,[17] missing polar interactions, and the flexible character of the compounds, the docking poses have to be interpreted with caution, but some assumptions can be derived. To summarize, the length of the linker seems to have an influence on the binding mode. Compounds with a C_5 and C_6 linker chain solely or preferentially exhibit a kinked position, in which the terminal phenyl residue overlaps the phenyl ring of covalent inhibitor **3** in the published crystal structure.[17] In contrast, compounds with a C_7 or C_8 linker show an extended conformation, in which the tetrazole moiety overlaps the position of the phenyl moiety of **3**.

Selectivity and stability studies

Another important enzyme in the process of endocannabinoid inactivation is monoacylglycerol lipase (MAGL). Similar to FAAH, MAGL contains a catalytic serine residue in the active site. The main substrate of MAGL is 2-arachidonoylglycerol. To obtain some information about the specificity of the developed substance class, phenyl carbamate **32** and pyridin-3-yl carbamate **59** were tested as representative examples for MAGL inhibition.[32] Whereas **32** did not affect the enzyme at the highest test concentration (10 μM), **59** was found to be an inhibitor of MAGL (IC$_{50}$: 0.50 μM). However, the inhibitory potency of this substance against FAAH was still 50-fold higher than that against MAGL. Similar results were found for structurally related phenyl and pyridin-3-yl *N*-indolylalkylcarbamates.[21]

Another enzyme of the serine hydrolase family is cytosolic phospholipase $A_2\alpha$ (cPLA$_2\alpha$), which catalyzes the first step of the so-called arachidonic acid cascade by cleaving membrane phospholipids into arachidonic acid and lysophospholipids. At the highest test concentration of 10 μM, cPLA$_2\alpha$ was not inhibited[33] by **32** and **59**. These results indicate that the inhibitors investigated display some specificity with regard to their ability to inhibit serine hydrolase enzymes.

Carbamates are known to be susceptible to chemical hydrolysis in aqueous solution as well as to enzymatic degradation in biological environments.[34–38] The chemical stabilities of compounds **32**, **34**, **45–47**, **51**, **54**, **59**, and **60** were tested (Table 6). In our FAAH assay, 0.2% Triton X-100 was added to the assay mixture to solubilize the fluorogenic FAAH substrate. In the chemical stability experiments, the test compounds were incubated in the presence of the same quantity of this detergent (0.2%) at a concentration of 20 μM at 37 °C for 60 min, centrifuged at 12 000 *g* for 5 min, and then directly subjected to HPLC/UV analysis. Upon comparing the amounts of the compounds present in these aqueous samples with their amounts in the freshly prepared reference solutions

(20 μM) in acetonitrile/PBS (1:1 *v/v*), it became evident that phenyl carbamates **32**, **34**, **45–47**, **51**, and **54** were all chemically stable under the conditions of the FAAH assay. Because the aqueous solutions were centrifuged before HPLC analysis, it could also be concluded that precipitation of the test compounds did not occur, which proved their solubility in the assay mixture even above the highest test concentration applied (10 μM). In contrast, the concentration of pyridin-3-yl carbamate **59** decreased to $(74\pm6)\%$ (mean $\pm$ SD, $n=3$) of the starting concentration within 60 min at 37 °C. In LC–MS(ESI+) experiments, beside the parent compound the formation of amine **61** by hydrolytic cleavage of **59** was detected. Additionally, a degradation product with $m/z=517.3$ [$M+H^+$] was detected, which clearly was a disubstituted urea derivative produced by reaction of amine **61** with **59** under substitution of pyridin-3-ol. These results indicate that the pyridin-3-yl carbamate moiety of **59** is more susceptible to nucleophilic attack by water than the phenyl carbamate group and, in the same way, to nucleophilic attack by the catalytic serine residue of the active site of FAAH. This could explain why the FAAH inhibitory activity of the pyridin-3-yl carbamates is significantly higher than that of the corresponding phenyl carbamates. The stability of pyridinyl carbamate **60** in aqueous solution could not be determined by HPLC/UV because the compound coeluted with UV-active matrix components.

Furthermore, we measured the stability of some of the new substances in rat liver S9 fractions as well as in porcine blood plasma with LC–MS (Table 6). After incubation in liver S9 fractions in the presence of the cofactor NADPH for 30 min, compound **45** with a pentyl spacer was degraded by ~40%. A similar metabolic rate was observed for a derivative of **45**, that is, compound **54**, in which the central carbon atom of the pentyl chain was replaced by an oxygen atom. Elongation of the pentyl chain led to an increase in the metabolic stability. From hexyl-, heptyl-, and octyl derivatives **32**, **46**, and **47**, ~70–90% of the parent compounds were still present after termination of the incubation in S9 fractions. High metabolic stabilities (~90%) were also measured in the case of a derivative of **32**, that is, compound **51**, in which four of the carbon atoms of the hexyl chain were replaced by a more rigid phenyl residue, and in the case of compound **34**, a chloro-substituted analogue of **32**. As shown by the data of **59** and **60**, replacement of the phenyl residue of the phenyl carbamate moiety by a pyridin-3-yl group decreased stability in the S9 fractions significantly. From the latter compounds, only ~40% was present after termination of the metabolic reactions. It must be kept in mind, however, that the hydrolytic liability of the pyridin-3-yl carbamate moiety of these compounds could contribute, at least in part, to their degradation under the conditions applied. In the LC–MS chromatograms of the phenyl carbamates, hydroxy metabolites were detectable, most likely produced by cytochrome P450 enzymes. In contrast, hydroxylated derivatives could not be found in the samples of the pyridin-3-yl carbamates.

In addition to oxidative metabolism, carbamates can be hydrolyzed to amines by esterases present in the liver homogenate. However, such cleavage products were not detected.

This could be due to the stability of these substances against the hydrolytic liver enzymes, or it could be the result of further degradation of the produced amines to aldehydes by amine oxidases (Scheme 7). Incubation of amines **61** and **63** showed that these compounds are not very stable in S9 fractions, similar to corresponding aldehydes **62** and **64**. Therefore, it is difficult to determine whether hydrolytic cleavage of the carbamates occurred during these experiments. The reference inhibitor URB 597 showed a high stability in S9 fractions. The lower value measured in previous experiments clearly was an artifact.[21]

Degradation of the carbamates was also observed in porcine plasma. The differences in the stabilities of the tested substances were even more pronounced than in the S9 fractions. Compounds **45**, **32**, **47**, and **51** with pentyl-, hexyl-, octyl-, and *para*-dimethylenephenyl spacers were degraded by ~40–50%. Interestingly, derivative **46** with a heptyl chain was significantly less stable. Approximately 80% of **46** disappeared after the incubation period of 30 min. In contrast, replacement of the central carbon atom of the pentyl chain of **45** by an oxygen atom to give **54** resulted in a considerable enhancement in stability. Nearly the entire amount of this substance was recovered from the plasma. An extreme liability in plasma was determined for pyridin-3-yl carbamates **59** and **60**. These two compounds were no longer detectable at the end of the 30 min incubation period. These results cannot be explained by the hydrolytic instability of the pyridin-3-yl carbamates in aqueous solution only, as ~75% of **59** remained intact in these experiments after an incubation time of even 60 min.

One reason for the observed instability of the carbamates in plasma could be their degradation by plasma esterases. Similar to human plasma, porcine plasma contains prominent amounts of butyrylcholine esterase (BChE) and paraoxonase (PON).[39–42] BChE is a serine esterase with a catalytic triad consisting of Ser, Glu, and His. In contrast, PON is not a member of the serine esterase family. It possesses a catalytic dyad comprising two histidine residues that are activated by binding of divalent calcium ions. In addition, some unknown esterases have been detected in porcine plasma. Moreover, esterase activity has also been reported for plasma albumin.[39, 43] To determine the agent responsible for the degradation of the carbamates, we first incubated the substances in the presence of porcine albumin. All phenyl carbamates proved to be stable under these conditions, whereas a pronounced decrease in the amounts of pyridin-3-yl carbamates **59** and **60** (~70%) was detected (Table 6). Next, we investigated whether selected compounds **46** and **59** could be stabilized by inhibitors of plasma

esterases. In these experiments, we used the highly potent BChE inhibitor rivastigmine[44] and the PON inhibitor ethylenediamine tetraacetic acid (EDTA).[45,46] Additionally, we measured the effect of bis(*p*-nitrophenyl)phosphate, as serine-reactive substance, which was reported to inhibit carboxylesterases.[45,46] As shown in Table 7, inhibition of BChE did not result
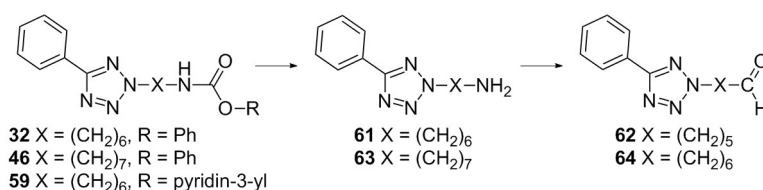
Table 7. Inhibition of the degradation of **46** and **59** in porcine plasma by esterase inhibitors.[a]

| Inhibitor	Conc.	Esterase	Inhibition [%][b]	
			46	**59**
Rivastigmine	100 μM	BChE	0	0
EDTA	1.5 mM	PON	28±12	9±4
BNPP	1 mM	CES	70±5	27±5
EDTA + BNPP	1.5 mM + 1 mM	PON + CES	88±3	33±11

[a] BNPP: bis(*p*-nitrophenyl)phosphate, BChE: butyrylcholine esterase, CES: carboxylesterase, PON: paraoxonase. [b] Values are the mean±SD, $n=3$.

in inhibition of the degradation of **46** and **59**. In contrast, the PON inhibitor EDTA decreased the conversions of **46** and **59** by 28 and 9%, respectively. The inhibitory effect of the carboxylesterase (CES) inhibitor bis(*p*-nitrophenyl)phosphate was even more pronounced: the transformations of **46** and **59** were decreased by 70 and 27%, respectively (Table 7). A combination of EDTA and bis(*p*-nitrophenyl)phosphate nearly completely inhibited metabolism of phenyl carbamate **46**, whereas pyridin-3-yl carbamate **59** was still degraded to a pronounced extent (~67%) in the presence of these two compounds. Taken together, these results show that BChE is not involved in metabolism of **46** and **59** in porcine plasma. In the case of compound **46**, PON and a CES-like enzyme (CESs themselves were not found in porcine blood[40]) were responsible for its cleavage. These two enzymes also participate in the degradation of **59**, but only by ~30%. The instability of this compound in pure porcine albumin solution makes its hydrolysis by the esterase activity of albumin probable or it reacts with the free amino or hydroxy groups of albumin to lead to covalent modification of albumin (Scheme 8).

The latter possibility was investigated by HPLC–MS(ESI).[47] The molecular weight of purified porcine albumin was determined from the well-resolved charge-state distribution to 66 875 Da (Figure 4). Incubating the protein with a fourfold molecular excess of compound **59** led to the formation of

32 X = (CH$_2$)$_6$, R = Ph
46 X = (CH$_2$)$_7$, R = Ph
59 X = (CH$_2$)$_6$, R = pyridin-3-yl

61 X = (CH$_2$)$_6$
63 X = (CH$_2$)$_7$

62 X = (CH$_2$)$_5$
64 X = (CH$_2$)$_6$

Scheme 7. Putative degradation of carbamates by hydrolases and amine oxidases.
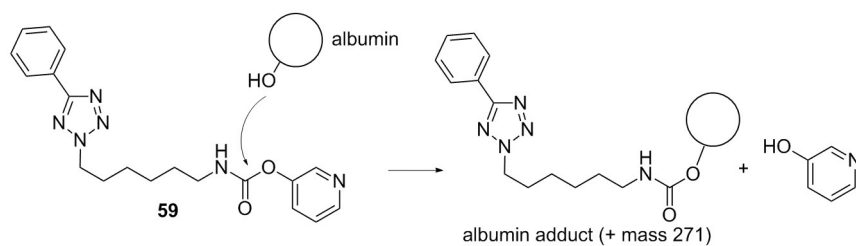
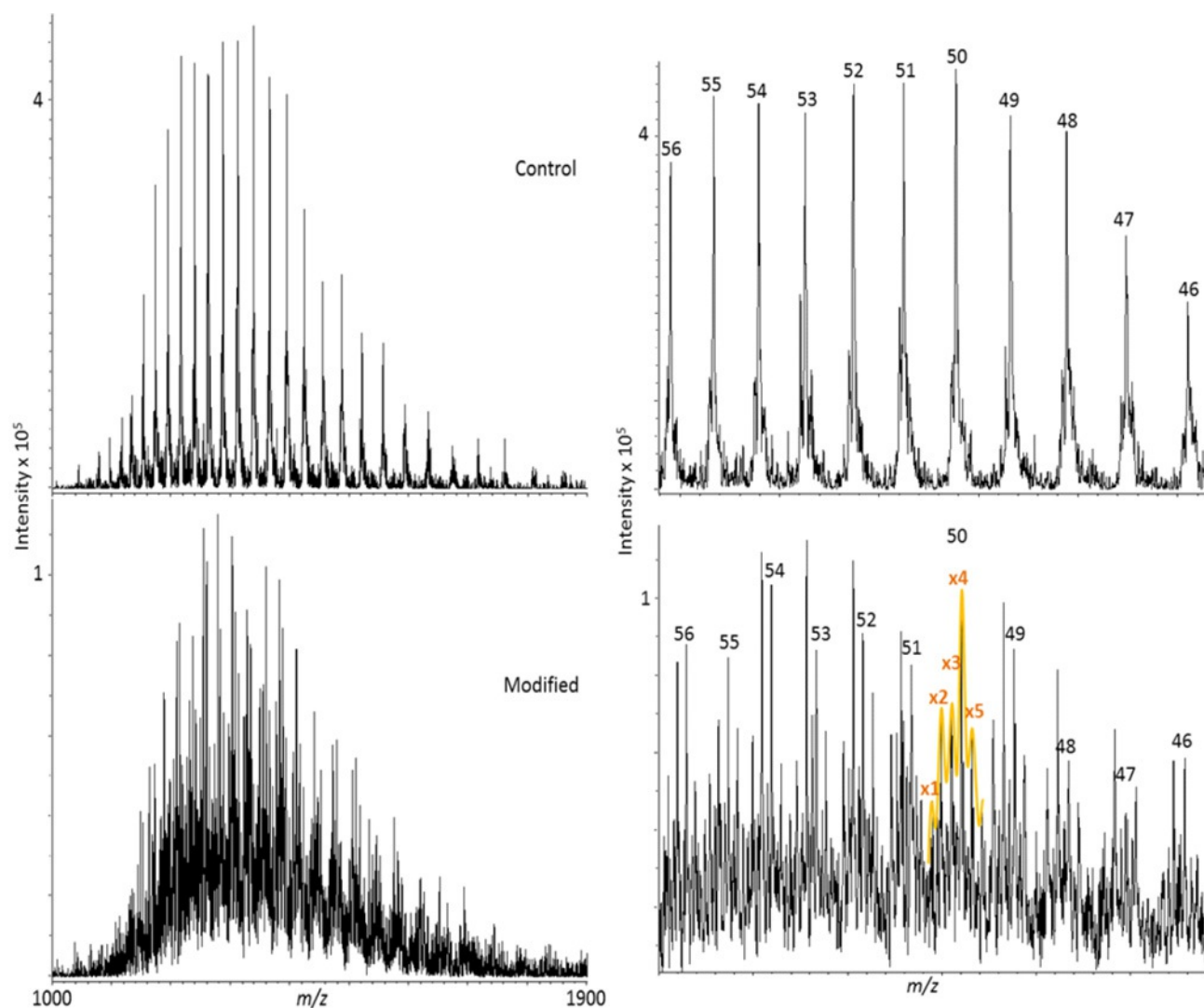**Scheme 8.** Proposed reaction of albumin with **59**.

Figure 4. Spectra for unmodified albumin (39.4–45 min; top) and albumin treated with **59** (40.8–50.5 min; bottom). Magnifications at right show the fine structure of the 11 most abundant charge states in the $m/z = 1200$–1500 range. The orange curve exemplarily marks the satellite peaks of protein forms with 50 charges. The addition of one to five molecules of the test substance is indicated.

a highly complex spectrum that was deconvoluted to show protein species of molecular weights 67 419, 67 689, 67 955, and 68 234 Da. This agrees with the expected multiple mass increase of 271 Da. The maximum peak distribution is noted for four molecules of the test compound. These results indicate that **59** is covalently bound to albumin during incubation in aqueous solution.

Conclusions

By systematic structural variation of phenyl *N*-[6-(2-methyl-4,5-diphenyl-1*H*-imidazol-1-yl)hexyl]carbamate (**2**), several potent phenyl and pyridin-3-yl carbamate inhibitors of FAAH were found. To rationalize the observed structure–activity relationships, docking experiments were performed. Reversibility stud-

ies indicated that the synthesized carbamates act by covalent modification of the enzyme. During the time span of the biological experiments, the phenyl carbamates were chemically stable, as shown for some selected compounds. In contrast, pyridin-3-yl *N*-[6-(5-phenyl-2*H*-tetrazol-2-yl)hexyl]carbamate (**59**) was cleaved hydrolytically to some extent. In rat liver homogenate and blood plasma, varying metabolic stabilities were measured. The significant liability of phenyl *N*-[7-(5-phenyl-2*H*-tetrazol-2-yl)heptyl]carbamate (**46**) in porcine plasma was due to cleavage by carboxylesterase-like serine hydrolases and paraoxonase. Pyridin-3-yl carbamate **59** was also degraded by these enzymes. However, additionally it clearly reacted directly with plasma albumin to lead to covalent adducts. Thus, despite its high FAAH inhibitory potency, pyridin-3-yl carbamate **59** does not seem to be suitable as a lead for further inhibitor development owing to its hydrolytic instability and its excessive off-target reactivity. The inhibitors with the best balance of activity, reactivity, and metabolic stability synthesized during this study are phenyl *N*-{6-[5-(3-chlorophenyl)-2*H*-tetrazol-2-yl]hexyl}carbamate (**34**) and phenyl *N*-[8-(5-phenyl-2*H*-tetrazol-2-yl)octyl]carbamate (**47**) (Table 6).

Experimental Section

Chemistry

General: Column chromatography was performed on silica gel 60, particle size 0.040–0.063 mm, from Macherey & Nagel. Melting points were determined with a Büchi B-540 apparatus. ^{1}H NMR spectra were recorded with a Varian Mercury Plus 400 spectrometer (400 MHz), Bruker AV300 spectrometer (300 MHz), or Bruker AV400 spectrometer (400 MHz). ^{13}C NMR spectra were measured with a Varian Mercury Plus 400 spectrometer (101 MHz). Electron ionization (EI) mass spectra were obtained with a Finnigan GCQ apparatus. High-resolution mass spectrometry (HRMS) was performed with a Bruker micrOTOF-Q II spectrometer by using electrospray ionization (ESI) or atmospheric pressure chemical ionization (APCI). The purity of the target compounds was assessed by reversed-phase (RP) HPLC on a Nucleosil 100 RP 18 3 μm column (3 mm inside diameter×125 mm). The samples were prepared by mixing a solution of 5 mм compound in DMSO (20 μL) with CH$_3$CN (180 μL). An aliquot (5 μL) of each solution was injected into the HPLC system. Elution was performed with a gradient consisting of CH$_3$CN/H$_2$O/trifluoroacetic acid (TFA) (42:58:0.1 to 86:14:0.1 *v/v/v*) or for amines **61** and **63** CH$_3$CN/10 mм ammonium acetate (10:90 to 90:10 *v/v*) adjusted to pH 5 with formic acid at a flow rate of 0.40 mL min^{-1}. UV absorbance was measured at $\lambda = 254$ nm. Purities of the target compounds were ≥95%.

The syntheses of target compounds **11**, **14**, **17 b**, **19–27**, **30**, **32–38**, **44**, **45–47**, **51**, and **54–60** are described in a patent application.[48]

2-[6-(4,5-Diphenyl-1*H*-imidazol-1-yl)hexyl]isoindoline-1,3-dione (7): Under a nitrogen atmosphere, potassium carbonate (314 mg, 2.27 mmol) was added to a solution of 4,5-diphenylimidazole (**6**; 250 mg, 1.13 mmol) in dry dimethyl sulfoxide (5 mL). After stirring the mixture at 60 °C for 15 min, a solution of *N*-(6-bromohexyl)phthalimide (352 mg, 1,13 mmol) in dry dimethyl sulfoxide (5 mL) was added and stirring was continued at 60 °C for 2 h. The resulting mixture was poured into H$_2$O (20 mL), acidified with dilute HCl to pH 6–7 and exhaustively extracted with CH$_2$Cl$_2$ (3×30 mL). The or-

ganic extracts were combined, washed with H$_2$O (2×50 mL), dried (Na$_2$SO$_4$), filtered, and concentrated. The crude material was purified by silica gel chromatography (hexane/EtOAc = 9:1 then EtOAc) to yield **7** as a solid (300 mg, 59%); mp: 105–107 °C; ^{1}H NMR (400 MHz, CDCl$_3$): $\delta = 1.20$-1.30 (m, 4H), 1.52-1.70 (m, 4H), 3.62 (t, $J = 7.1$ Hz, 2H), 3.95 (t, $J = 7.4$ Hz, 2H), 7.24-7.29 (m, 3H), 7.32-7.37 (m, 2H), 7.48-7.56 (m, 5H), 7.70-7.73 (m, 2H), 7.82-7.86 (m, 2H), 8.57 ppm (s, 1H); MS (EI, 70 eV): *m/z* (%): 449 (100) [*M*$^+$], 372 (60).

Phenyl *N*-[6-(4,5-diphenyl-1*H*-imidazol-1-yl)hexyl]carbamate (8): Hydrazine hydrate (24% *w/w*, 760 μL) was added to a solution of **7** (275 mg, 0.61 mmol) in EtOH (30 mL), and the mixture was heated at reflux for 2 h. The solvent was evaporated, and the resulting residue was treated with brine (30 mL). After adjusting the pH value of the mixture to ~10 with dilute NaOH, the solution was extracted exhaustively with CHCl$_3$ (3×30 mL), dried (Na$_2$SO$_4$), filtered, and concentrated to give 6-(4,5-diphenyl-1*H*-imidazol-1-yl)hexan-1-amine (194 mg, 99%). This intermediate (194 mg, 0.61 mmol) was dissolved in dry THF (7 mL) and then Et$_3$N (112 μL) and phenyl chloroformate (128 mg, 103 μL, 0.82 mmol) were added dropwise. The resulting solution was stirred at RT for 1.5 h. The mixture was poured into H$_2$O (20 mL) and exhaustively extracted with CH$_2$Cl$_2$ (3×30 mL). The organic layers were combined, dried (Na$_2$SO$_4$), filtered, and concentrated. The crude product was purified by silica gel chromatography (CH$_2$Cl$_2$/EtOAc = 8:2) to yield **8** as a solid (70 mg, 26%); mp: 124–125 °C; ^{1}H NMR (400 MHz, [D$_6$]DMSO): $\delta = 1.04$-1.21 (m, 4H), 1.28-1.39 (m, 2H), 1.40-1.53 (m, 2H), 2.90-3.10 (m, 2H), 3.80 (t, $J = 7.2$ Hz, 2H), 7.04-7.12 (m, 3H), 7.14-7.22 (m, 3H), 7.32-7.41 (m, 6H), 7.45-7.55 (m, 3H), 7.71 (t, $J = 5.6$ Hz, 1H), 7.84 ppm (s, 1H); ^{13}C NMR (101 MHz, [D$_6$]DMSO): $\delta = 25.5$, 25.5, 29.0, 29.9, 40.3, 44.3, 121.8, 124.9, 125.9, 126.0, 128.1, 128.1, 128.8, 129.2, 129.3, 130.7, 130.9, 135.0, 136.7, 137.5, 151.1, 154.3 ppm; HRMS (ESI): *m/z*: calcd for C$_{28}$H$_{29}$N$_3$O$_2$: 440.2333 [*M*+H$^+$]; found: 440.2327.

tert-Butyl 4-(2*H*-tetrazol-5-yl)benzoate (40): A mixture of *tert*-butyl 4-cyanobenzoate[49] (**39**; 215 mg, 1.06 mmol), trimethylsilyl azide (244 mg, 2.11 mmol), and tetrabutylammonium fluoride hydrate (138 mg, 0.53 mmol) was heated at 120 °C for 3 h. After the addition of THF (30 mL) and silica gel (6 g), the mixture was concentrated to dryness. The residue was put on top of a silica gel column and chromatographed (hexane/EtOAc = 6:4, then hexane/EtOAc/formic acid = 6:4:0.1) to yield **40** as a solid (226 mg, 87%); mp: 293 °C (decomp.); ^{1}H NMR (400 MHz, [D$_6$]DMSO): $\delta = 1.57$ (s, 9H), 8.08-8.13 (m, 2H), 8.14-8.19 ppm (m, 2H); HRMS (APCI): *m/z* calcd for C$_{12}$H$_{14}$N$_4$O$_2$: 247.1190 [*M*+H$^+$]; found: 247.1203.

tert-Butyl 4-{2-[6-(1,3-dioxoisoindolin-2-yl)hexyl]-2*H*-tetrazol-5-yl}benzoate (41): Compound **41** was prepared from **40** (197 mg, 0.80 mmol) in a manner similar to that described for the preparation of **7**. After purification by silica gel chromatography (hexane/EtOAc = 8:2), the product was afforded as a solid (281 mg, 74%); mp: 70–73 °C; ^{1}H NMR (400 MHz, [D$_6$]DMSO): $\delta = 1.28$–1.37 (m, 4H), 1.54-1.61 (m, 11H), 1.92-2.01 (m, 2H), 3.55 (t, $J = 7.1$ Hz, 2H), 4.74 (t, $J = 7.0$ Hz, 2H), 7.79-7.87 (m, 4H), 8.04-8.08 (m, 2H), 8.15-8.19 ppm (m, 2H); HRMS (APCI): *m/z* calcd for C$_{29}$H$_{29}$N$_5$O$_4$: 476.2292 [*M*+H$^+$]; found: 476.2374.

tert-Butyl 4-(2-{6-[(phenoxycarbonyl)amino]hexyl}-2*H*-tetrazol-5-yl)benzoate (42): Hydrazine hydrate (24% *w/w*, 486 μL) was added to a solution of **41** (140 mg, 0.29 mmol) in EtOH (30 mL), and the mixture was heated at reflux for 2 h. The solvent was evaporated, and the resulting residue was treated with brine (30 mL). After adjusting the pH value to ~10 with dilute NaOH, the solution was extracted exhaustively with CHCl$_3$ (3×30 mL), dried (Na$_2$SO$_4$), filtered,

and concentrated to give *tert*-butyl 4-[2-(6-aminohexyl)-2*H*-tetrazol-5-yl]benzoate. This intermediate (102 mg, 0.30 mmol) was dissolved in dry THF (7 mL) and then ethyl(diisopropyl)amine (57 μL) and phenyl chloroformate (53 mg, 42 μL, 0.34 mmol) were added dropwise. The resulting solution was stirred at RT for 5 h. Then, the mixture was poured into H_2O (20 mL) and extracted exhaustively with CH_2Cl_2 (3×30 mL). The organic layers were combined, dried (Na_2SO_4), filtered, and concentrated. The crude product was purified by silica gel chromatography (hexane/EtOAc = 8:2 to 7:3) to yield **42** as a solid (116 mg, 83 %); mp: 91–92 °C; ^{1}H NMR (400 MHz, [D_6]DMSO): δ = 1.26-1.40 (m, 4H), 1.40-1.51 (m, 2H), 1.57 (s, 9H), 1.93-2.04 (m, 2H), 3.00-3.17 (m, 2H), 4.77 (t, *J* = 7.0 Hz, 2H), 7.07 (d, *J* = 8.0 Hz, 2H), 7.18 (t, *J* = 7.4 Hz, 1H), 7.36 (t, *J* = 7.9 Hz, 2H), 7.72 (t, *J* = 5.5 Hz, 1H), 8.07 (d, *J* = 8.3 Hz, 2H), 8.18 ppm (d, *J* = 8.3 Hz, 2H); HRMS (APCI): *m/z* calcd for $C_{25}H_{31}N_5O_4$: 466.2449 [*M*+H$^+$]; found: 466.2526.

4-(2-{6-[(Phenoxycarbonyl)amino]hexyl}-2*H*-tetrazol-5-yl)benzoic acid (43): TFA (1.0 mL, 13.1 mmol) was added dropwise to a solution of **42** (108 mg, 0.23 mmol) in dry CH_2Cl_2 (20 mL) under an atmosphere of nitrogen at 0 °C. The mixture was stirred at RT for 24 h. Then, the solvent was evaporated. To remove remaining TFA, CH_2Cl_2 was added and then distilled (2×) to yield **43** as a solid (94 mg, 99 %); mp: 189–190 °C; ^{1}H NMR (400 MHz, [D_6]DMSO): δ = 1.27-1.40 (m, 4H), 1.41-1.52 (m, 2H), 1.92-2.05 (m, 2H), 2.96-3.17 (m, 2H), 4.77 (t, *J* = 7.0 Hz, 2H), 7.05-7.11 (m, 2H), 7.18 (t, *J* = 7.4 Hz, 1H), 7.32-7.39 (m, 2H), 7.72 (t, *J* = 5.5 Hz, 1H), 8.09-8.13 (m, 2H), 8.16-8.21 (m, 2H), 13.22 ppm (s, 1H); ^{13}C NMR (101 MHz, [D_6]DMSO): δ = 25.4, 25.5, 28.6, 28.9, 40.3, 52.9, 121.7, 124.8, 126.5, 129.2, 130.2, 130.8, 132.3, 151.1, 154.3, 163.3, 166.7 ppm; HRMS (ESI): *m/z* calcd for $C_{21}H_{23}N_5O_4$: 410.1823 [*M*+H$^+$]; found: 410.1849.

6-(5-Phenyl-2*H*-tetrazol-2-yl)hexan-1-amine (61): A mixture of 5-phenyltetrazole (213 mg, 1.46 mmol), *N*-(6-bromohexyl)phthalimide (465 mg, 1.50 mmol), K_2CO_3 (415 mg, 3.0 mmol), and dry CH_3CN (20 mL) was heated at reflux for 3 h. The mixture was diluted with EtOAc (30 mL), filtered, and concentrated. The residue was dissolved in a small amount of toluene/CH_2Cl_2 (3 mL) and chromatographed on silica gel (hexane/EtOAc = 8:2) to yield 2-[6-(5-phenyl-2*H*-tetrazol-2-yl)hexyl]isoindoline-1,3-dione (393 mg, 72 %). This intermediate (393 mg, 1.05 mmol) was dissolved in EtOH (25 mL), hydrazine hydrate (24 % *w/w*, 1.8 mL) was added, and the mixture was heated at reflux for 3 h. The solvent was evaporated, and the resulting residue was treated with brine (30 mL). After adjusting the pH value of the mixture to ~10 with dilute NaOH, the solution was extracted exhaustively with $CHCl_3$ (3×30 mL), dried (Na_2SO_4), filtered, and concentrated to yield **61** as a waxy compound (230 mg, 89 %). ^{1}H NMR (400 MHz, CDCl$_3$): δ = 1.35–1.43 (m, 4H), 1.43–1.49 (m, 2H), 1.52–1.68 (m, 2H), 2.04–2.11 (m, 2H), 2.69 (t, *J* = 6.6 Hz, 2H), 4.65 (t, *J* = 7.1 Hz, 2H), 7.44–7.53 (m, 3H), 8.11–8.18 ppm (m, 2H); ^{13}C NMR (101 MHz, CDCl$_3$): δ = 26.3, 29.5, 33.4, 42.1, 53.2, 126.9, 127.7, 129.0, 130.4, 165.2 ppm; HRMS (APCI): *m/z* calcd for $C_{13}H_{19}N_5$: 246.1713 [*M*+H$^+$]; found: 246.1734.

6-(5-Phenyl-2*H*-tetrazol-2-yl)hexanal (62): A solution of 5-phenyltetrazole (292 mg, 2.00 mmol) in propan-2-ol (6 mL) was treated with powdered KOH (88 %, 112 mg, 1.76 mmol) and then heated at reflux for 1 h. A solution of 6-bromohexan-1-ol (362 mg, 2.00 mmol) in propan-2-ol (6 mL) was then added and heating was continued for 9 h. The solvent was distilled off and the residue was treated with H_2O (150 mL). The resulting mixture was extracted with CH_2Cl_2 (70 mL). The organic layer was dried (Na_2SO_4), filtered, and concentrated. The residue was dissolved in a small amount of toluene and chromatographed on silica gel (cyclohexane/EtOAc = 7:3) to yield 6-(5-phenyl-2*H*-tetrazol-2-yl)hexan-1-ol (197 mg, 40 %).

Under a nitrogen atmosphere, this intermediate (95 mg, 0.39 mmol) was dissolved in dry CH_2Cl_2 (10 mL) and Dess–Martin periodinane (245 mg, 0.58 mmol) was added. The mixture was stirred at RT for 3 h. Then, a solution of $Na_2S_2O_3$ (1 g) in a saturated aqueous $NaHCO_3$ solution (20 mL) was added. The mixture was stirred for 5 min, diluted with H_2O, and extracted with CH_2Cl_2 (2× 50 mL). The combined organic layer was dried (Na_2SO_4), filtered, and concentrated. The residue was dissolved in a small amount of toluene and chromatographed on silica gel (cyclohexane/EtOAc = 8:2) to yield **62** as an oil (51 mg, 54 %). Data for 6-(5-phenyl-2*H*-tetrazol-2-yl)hexan-1-ol: ^{1}H NMR (400 MHz, CDCl$_3$): δ = 1.36–1.50 (m, 4H), 1.52–1.64 (m, 2H), 2.08 (quint., *J* = 7.1 Hz, 2H), 3.64 (t, *J* = 6.4 Hz, 2H), 4.66 (t, *J* = 7.1 Hz, 2H), 7.45–7.52 (m, 3H), 8.11–8.18 ppm (m, 2H); ^{13}C NMR (101 MHz, CDCl$_3$): δ = 25.2, 26.3, 29.5, 32.5, 53.2, 62.8, 126.9, 127.6, 129.1, 130.4, 165.2 ppm; HRMS (APCI): *m/z* calcd for $C_{13}H_{18}N_4O$: 247.1553 [*M*+H$^+$]; found: 247.1551. Data for **62**: ^{1}H NMR (400 MHz, CDCl$_3$): δ = 1.34–1.46 (m, 2H), 1.63–1.77 (m, 2H), 2.00–2.14 (m, 2H), 2.46 (td, *J* = 1.5, 7.2 Hz, 2H), 4.66 (t, *J* = 7.0 Hz, 2H), 7.43–7.53 (m, 3H), 8.09–8.17 (m, 2H), 9.76 ppm (t, *J* = 1.5 Hz, 1H); ^{13}C NMR (101 MHz, CDCl$_3$): δ = 21.3, 25.9, 29.1, 43.5, 52.8, 126.8, 127.4, 128.9, 130.2, 165.1, 201.9 ppm. HRMS (ESI): *m/z* calcd for $C_{13}H_{16}N_4O$: 245.1397 [*M*+H$^+$]; found: 245.1464.

7-(5-Phenyl-2*H*-tetrazol-2-yl)heptan-1-amine (63): A solution of 5-phenyltetrazole (292 mg, 2.00 mmol) in propan-2-ol (6 mL) was treated with powdered KOH (88 %, 112 mg, 1.76 mmol) and heated at reflux for 1 h. Then, a solution of 1,6-dibromoheptane (1.89 g, 1.25 mL, 7.32 mmol) in propan-2-ol (6 mL) was added and heating was continued for 7 h. The solvent was distilled off, and the residue was chromatographed on silica gel (cyclohexane/EtOAc = 9:1) to yield 1-bromo-7-(5-phenyl-2*H*-tetrazol-2-yl)heptane (330 mg, 51 %). A mixture of this intermediate (310 mg, 0.96 mmol), potassium phthalimide (178 mg, 0.96 mmol), K_2CO_3 (1.4 g, 10 mmol), and CH_3CN (10 mL) was heated at reflux for 14 h. After the addition of H_2O (150 mL), the mixture was extracted with EtOAc (70 mL). The organic layer was dried (Na_2SO_4), filtered, and concentrated. The residue was chromatographed on silica gel (cyclohexane/EtOAc = 9:1 to 8:2) to yield 2-[7-(5-phenyl-2*H*-tetrazol-2-yl)heptyl]isoindoline-1,3-dione (74 mg, 20 %). This intermediate (74 mg, 0.19 mmol) was dissolved in EtOH (5 mL) and hydrazine hydrate (24 % *w/w*, 1.0 mL) was added. The mixture was heated at reflux for 3 h. The solvent was evaporated, and the resulting residue was treated with brine (30 mL). After adjusting the pH value of the mixture to ~10 with dilute NaOH, the solution was extracted exhaustively with CH_2Cl_2 (3×30 mL), dried (Na_2SO_4), filtered, and concentrated to yield **63** as a waxy substance (47 mg, 95 %). Data for 1-bromo-7-(5-phenyl-2*H*-tetrazol-2-yl)heptane: ^{1}H NMR (300 MHz, CDCl$_3$): δ = 1.33–1.51 (m, 6H), 1.85 (quint., *J* = 6.9 Hz, 2H), 2.01–2.13 (m, 2H), 3.40 (t, *J* = 6.8 Hz, 2H), 4.65 (t, *J* = 7.1 Hz, 2H), 7.43–7.53 (m, 3H), 8.11–8.18 ppm (m, 2H); HRMS (ESI): *m/z* calcd for $C_{14}H_{19}BrN_4$: 323.0866 [*M*+H$^+$]; found: 323.0865. Data for **63**: ^{1}H NMR (400 MHz, CDCl$_3$): δ = 1.28–1.39 (m, 6H), 1.40–1.48 (m, 2H), 1.60–1.77 (m, 2H), 2.03–2.10 (m, 2H), 2.66–2.72 (m, 2H), 4.64 (t, *J* = 7.1 Hz, 2H), 7.45–7.52 (m, 3H), 8.12–8.17 ppm (m, 2H); ^{13}C NMR (101 MHz, CDCl$_3$): δ = 26.5, 26.8, 28.9, 29.5, 33.5, 42.1, 53.3, 126.9, 127.7, 129.0, 130.4, 165.2; HRMS (ESI): *m/z* calcd for $C_{14}H_{21}N_5$: 260.1870 [*M*+H$^+$]; found: 260.1866.

7-(5-Phenyl-2*H*-tetrazol-2-yl)heptanal (64): 5-Phenyltetrazole (292 mg, 2.00 mmol) was treated with 7-bromoheptan-1-ol (390 mg, 2.00 mmol) by using the procedure described above for the synthesis of 6-(5-phenyl-2*H*-tetrazol-2-yl)hexan-1-ol. The reaction time was 15 h. An aliquot of the obtained intermediate, 7-phenyl-2*H*-tetrazol-2-yl)heptan-1-ol (148 mg, 0.57 mmol), was oxi-

dized with Dess–Martin periodinane following the same procedure as that described for the synthesis of **62** to yield **64** as an oil (90 mg, 61%). ^{1}H NMR (400 MHz, CDCl$_3$): $\delta = 1.35$–1.45 (m, 4H), 1.60–1.68 (m, 2H), 2.01–2.12 (m, 2H), 2.43 (td, $J = 7.2$, 1.6 Hz, 2H), 4.65 (t, $J = 7.1$ Hz, 2H), 7.44–7.52 (m, 3H,), 8.12–8.17 (m, 2H), 9.75 ppm (t, $J = 1.7$ Hz, 1H). ^{13}C NMR (101 MHz, CDCl$_3$): $\delta = 21.9$, 26.3, 28.5, 29.3, 43.8, 53.2, 127.0, 127.6, 129.0, 130.4, 165.2, 202.5 ppm. HRMS (ESI): m/z calcd for C$_{14}$H$_{18}$N$_4$: 259.1553 [$M+H^+$]; found: 259.1558.

Biological and chemical assays

Materials: PBS solution prepared from PBS tablets (one tablet dissolved in 200 mL deionized water yields 0.01 M phosphate buffer, 0.0027 M KCl and 0.137 M NaCl, pH 7.4, 25 °C), dimethyl sulfoxide (DMSO), porcine albumin, bis(*p*-nitrophenyl)phosphate (Sigma–Aldrich), MeOH (HPLC grade), CH$_3$CN (HPLC grade), EDTA (VWR), rivastigmine (Toronto Research Chemicals/Biozol), livers of female Wistar rats (Pharmacological section of the Institute of Pharmaceutical and Medicinal Chemistry, University of Münster), porcine blood (Schlachthof Tummel, Schöppingen or Feinkostfleischerei Hidding, Nordwalde).

Inhibition of FAAH: Inhibition of FAAH was measured with FAAH as described.[28] Briefly, the substrate *N*-(2-hydroxyethyl)-4-pyren-1-yl-butanamide (100 μM) solubilized with Triton X-100 (0.2%) was incubated with rat brain microsomes. FAAH activity was determined directly without further sample clean up by measuring the amount of 4-pyren-1-ylbutanoic acid released by FAAH in the absence and presence of a test compound by RP HPLC and fluorescence detection. Deviating from this published procedure, the incubation was performed in Tris buffer (50 mM Tris-HCl, containing 1 mM sodium EDTA and adjusted to pH 7.4 at 20 °C) instead of PBS, and the incubation time was 60 min instead of 45 min. These alterations led to slight divergences of the IC$_{50}$ values obtained for the reference inhibitors URB 597 (**1**) and BMS-1 (**2**) from the published data.[21,28]

FAAH reversibility studies: A rat brain microsomal preparation (9.5 μL),[28] previously freshly homogenized by sonication (Branson sonifier B15, 2×5 s at 0 °C), was added to DMSO (in the case of the control incubations) (0.5 μL) or a DMSO solution of the test compound (**46** and **59**, respectively) (0.5 μL) (concentration range: 0.02–2.0 μM). The samples were incubated at 37 °C for 60 min and then rapidly diluted with a mixture (88:2 *v/v*) of a solution of 0.2% Triton X-100 in PBS containing EDTA (1 mM) and the FAAH substrate *N*-(2-hydroxyethyl)-4-pyren-1-ylbutanamide in DMSO (5 mM) (90 μL). The final test compound concentration ranged from 1 to 100 nM, and the substrate concentration was 100 μM. The incubation at 37 °C was continued for 60 min. Then, the enzyme reaction was terminated by the addition of CH$_3$CN/MeOH (1:1 *v/v*, 200 μL), which contained the internal standard 6-pyren-1-ylhexanoic acid (0.025 μg/200 μL). After cooling in an ice bath for 10 min, the samples were centrifuged at 2000 g at 4 °C for 5 min and subjected to HPLC analysis as described previously.[28]

In the same manner, DMSO solutions of **46** and **59** were pre-incubated with the rat brain microsomal preparation at 37 °C for 60 min. Then, the samples were diluted rapidly with a solution of 0.2% Triton X-100 in PBS (88 μL) containing EDTA (1 mM). Incubation at 37 °C was continued for 60 min. Only then was the enzyme reaction started by the addition of a DMSO solution of the substrate (5 mM, 2 μL). After incubation for another 60 min, enzymatic substrate cleavage was terminated and the samples were analyzed by HPLC as described above. To calculate enzyme inhibition, the ratio of the peaks of the enzyme product and the internal standard

obtained in the presence of a test compound was compared with the mean level of this peak ratio determined in the absence of the test compounds (i.e., control tests, $n = 3$). In parallel, the IC$_{50}$ values of **46** and **59** were determined in PBS without pre-incubation of the enzyme and inhibitor as previously described[28] by using an incubation time of 60 min.

Inhibition of monoacylglycerol lipase (MAGL): The effect of selected compounds on the activity of the endocannabinoid-degrading enzyme monoacylglycerol lipase (MAGL) was evaluated as previously described by using human recombinant MAGL.[21,32] Briefly, the substrate 1,3-dihydroxypropan-2-yl 4-pyren-1-ylbutanoate was solubilized with Triton X-100 (0.2%). The enzyme reaction was terminated after 45 min by adding a mixture of CH$_3$CN/MeOH including the internal standard 6-pyren-1-ylhexanoic acid. MAGL inhibition by the test compounds was determined by measuring the amount of 4-pyren-1-ylbutanoic acid released by the enzyme in the absence and presence of the test compound by RP HPLC with fluorescence detection.

Inhibition of cytosolic phospholipase A$_2\alpha$ (cPLA$_2\alpha$): Inhibition of cPLA$_2\alpha$ was measured according to a recently published procedure.[33] Briefly, cPLA$_2\alpha$ isolated from porcine platelets was incubated with co-vesicles consisting of the substrate 1-stearoyl-2-arachidonoyl-*sn*-glycero-3-phosphocholine (200 μM) and 1,2-dioleoyl-*sn*-glycerol (100 μM). Enzyme reactions were terminated after 60 min, and cPLA$_2\alpha$ activity was determined by measuring arachidonic acid released by the enzyme in the absence and presence of a test compound by RP HPLC and UV detection at $\lambda = 200$ nm after online solid-phase extraction.

Chemical stability and solubility in aqueous solution: Adapting the conditions of the FAAH assay,[28] a solution of the test compound in DMSO (5 mM, 2 μL) was diluted with a solution of 0.2% Triton X-100 in PBS (98 μL) containing EDTA (1 mM) and incubated at 37 °C for 60 min. Immediately thereafter, the sample was centrifuged at 12 000 g and 20 °C for 5 min and analyzed by HPLC. Separation was achieved on a Dionex HPLC apparatus (Thermo Scientific) by using a Nucleosil C$_{18}$ analytical column (3 mm inside diameter × 125 mm, particle size 3 μm, Macherey & Nagel) protected with a Phenomenex C$_{18}$ guard column (3 mm inside diameter × 4 mm). An aliquot of the samples (30 μL) was injected into the HPLC system. Autosampler and column oven temperature were set to 20 °C. The mobile phase consisted of CH$_3$CN/aqueous ammonium acetate (10 mM, 58:42 *v/v*) adjusted to pH 5.0 with formic acid. The flow rate was 0.4 mL min^{-1} and the absorption wavelength was set to 238 nm. The relative amount of the test compound found in the aqueous sample after 60 min incubation at 37 °C was determined with the aid of a freshly prepared reference solution obtained by dilution of a DMSO solution (5 mM) of the compound (2 μL) with CH$_3$CN/PBS (1:1 *v/v*, 98 μL).

Metabolic stability in rat liver S9 fractions: The metabolic stability was tested by using S9 fractions of rat liver homogenate.[28] Briefly, the test compounds were incubated under aerobic conditions in the presence of the cofactor NADPH. The metabolic reactions were terminated after 30 min by the addition of CH$_3$CN. Controls were prepared by the addition of the test compounds to a mixture of S9 fractions and CH$_3$CN. In deviation to the published procedure, the extent of metabolism was evaluated by RP HPLC with MS detection. The HPLC–MS system from Shimadzu (Kyoto, Japan) consisted of two LC-20ADXR HPLC-pumps, a SIL-30AC autosampler, and a LC–MS-2020 single quad detector. Aliquots (2 μL) were injected onto a HICHROM ACE 3 C$_{18}$ column (2.1 mm inside diameter × 100 mm, particle size 3 μm) protected with a Phenomenex C$_{18}$

guard column (3 mm inside diameter×4 mm). Autosampler temperature was 10 °C, column oven temperature was set to 30 °C. The mobile phase consisted of CH$_3$CN/10 mm ammonium acetate 10:90 v/v, adjusted to pH 5 with formic acid (A), and CH$_3$CN/10 mm ammonium acetate 90:10 v/v, adjusted to pH 5 with formic acid. The following gradient was applied for solvent A: 0 min: 90%; 1 min: 90%; 9 min: 0%; 11 min: 0%; 11.5 min: 90%; 16 min: 90%. The flow rate was 0.2 mL min^{-1}. Detection was performed in ESI+ mode. Samples and controls of each test compound were processed and analyzed in rapid succession.

Metabolic stability in porcine plasma: A solution of the test compound (5 mm) in DMSO (1 μL) was added to a mixture of porcine plasma (125 μL) and PBS (124 μL). After incubation at 37 °C for 30 min, CH$_3$CN (500 μL) was added. The mixture was vortexed and allowed to stand in an ice bath for 15 min. After vigorous vortexing, the mixture was centrifuged at 12 000 g and 4 °C for 5 min. In parallel, controls were prepared by adding the DMSO solution (5 mm) of the test compound (1 μL) to a mixture of porcine plasma (125 μL), PBS (124 μL), and CH$_3$CN (500 μL). The controls were allowed to stand at RT for 30 min. Then, they were cooled in an ice bath for 15 min, vigorously vortexed, and centrifuged at 12 000 g and 4 °C for 5 min. The supernatants of the samples were separated and analyzed by HPLC–MS as described above. Samples and controls of each test compound were processed and analyzed in rapid succession. The inhibition experiments were performed in the same manner with the following modifications: In the incubations with rivastigmine and bis(p-nitrophenyl)phosphate, the amount of PBS was decreased to 123 μL, and 1 μL of a DMSO solution with rivastigmine (25 mm) or bis(p-nitrophenyl)phosphate (250 mm) was added additionally. In the experiments with DMSO, PBS (124 μL) was replaced by a solution of EDTA (3 mm) in PBS (123 μL) and DMSO (1 μL).

Stability in porcine albumin solution: A solution of the test compound (5 mm) in DMSO (1 μL) was added to a solution of porcine albumin (17.5 mg mL^{-1}) in PBS (249 μL). After incubation at 37 °C for 30 min, CH$_3$CN (500 μL) was added. The mixture was vortexed and allowed to stand in an ice bath for 15 min. After vigorous vortexing, the mixture was centrifuged at 12 000 g and 4 °C for 5 min. In parallel, controls were prepared by adding the DMSO solution (5 mm) of the test compound (1 μL) to a solution of porcine albumin (17.5 mg mL^{-1}) in PBS (249 μL) and CH$_3$CN (500 μL). The controls were allowed to stand at RT for 30 min. Then, they were cooled in an ice bath for 15 min, vigorously vortexed, and centrifuged at 12 000 g and 4 °C for 5 min. The supernatants of the samples were separated and analyzed by HPLC–MS as described above. Samples and controls of each test compound were processed and analyzed in rapid succession.

*Determination of the reaction of **59** with porcine albumin by MS*: A solution of porcine albumin (35 mg mL^{-1}) in PBS (0.01 m, 25 μL) was diluted with PBS (0.01 m, 215 μL). Then, a solution of compound **59** (5 mm) in DMSO (10 μL) was added, and the mixture was incubated at 37 °C for 60 min (molar ratio compound **59**/albumin = 4:1). In the same way, a reference solution was prepared by using pure DMSO instead of the DMSO solution of **59**. Mass spectrometry determination of the molecular weight of intact proteins was performed as previously described[47] by using RP HPLC on HP1100 (Agilent) coupled to an Esquire 3000 ion trap (Bruker Daltonics). To that end, the sample (9 μL) was injected for measurement in positive-ion mode. Accumulated spectra were manually deconvoluted by using the most intense peaks of each charge-state distribution.

Docking studies

A target model was created by using the crystal structure of α-keto heterocycle inhibitor **3** bound to a variant of FAAH (PDB ID: 3K7F).[17] Solvent, B-chain, and bound ligand of the X-ray structure were removed. Then, the model of truncated FAAH was protonated by using Protonate 3D from the program MOE[50] and manually deprotonated at the oxygen atom of the Ser241 residue. This structure was used as a target structure for all docking runs, which were performed with GOLD.[51] For covalent docking, the structures of the test compounds were manually transformed into the tetrahedral form of the transition state formed during a reaction of covalent carbamate inhibitors with a catalytic serine by using MOE. The oxygen atom of the Ser241 residue was defined as a protein link. Topology matching was used to check test equivalent atoms. The docking experiments were performed with a maximum of 15 different poses, which were created with genetic algorithm settings, set to automatic and 200% search efficiency, and using ChemScore as scoring function. The docking run for a single compound was stopped if three poses were within an RMSD of 1.5 Å (early termination option). Pictures were created by using UCSF Chimera.[52]

[1] C. J. Fowler, *Fundam. Clin. Pharmacol.* **2006**, *20*, 549–562.
[2] V. Di Marzo, *Rev. Physiol. Biochem. Pharmacol.* **2008**, *160*, 1–24.
[3] A. C. Howlett, F. Barth, T. I. Bonner, G. Cabral, P. Casellas, W. A. Devane, C. C. Felder, M. Herkenham, K. Mackie, B. R. Martin, R. Mechoulam, R. G. Pertwee, *Pharmacol. Rev.* **2002**, *54*, 161–202.
[4] S. D. McAllister, M. Glass, *Prostaglandins Leukotrienes Essent. Fatty Acids* **2002**, *66*, 161–171.
[5] E. S. Graham, J. C. Ashton, M. Glass, *Front. Biosci., Landmark Ed.* **2009**, *14*, 944–957.
[6] M. K. McKinney, B. F. Cravatt, *Annu. Rev. Biochem.* **2005**, *74*, 411–432.
[7] G. Labar, C. Michaux, *Chem. Biodiversity* **2007**, *4*, 1882–1902.
[8] F. Fezza, C. De Simone, D. Amadio, M. Maccarrone, *Subcell. Biochem.* **2008**, *49*, 101–132.
[9] K. Ahn, M. K. McKinney, B. F. Cravatt, *Chem. Rev.* **2008**, *108*, 1687–1707.
[10] S. M. Saario, J. T. Laitinen, *Basic Clin. Pharmacol. Toxicol.* **2007**, *101*, 287–293.
[11] S. Vandevoorde, *Curr. Top. Med. Chem.* **2008**, *8*, 247–267.
[12] K. Ahn, D. S. Johnson, B. F. Cravatt, *Expert Opin. Drug Discovery* **2009**, *4*, 763–784.
[13] H. Deng, *Expert Opin. Drug Discovery* **2010**, *5*, 961–993.
[14] I. K. Khanna, C. W. Alexander, *CNS Neurol. Disord. Drug Targets* **2011**, *10*, 545–558.
[15] S. Kathuria, S. Gaetani, D. Fegley, F. Valino, A. Duranti, A. Tontini, M. Mor, G. Tarzia, G. La Rana, A. Calignano, A. Giustino, M. Tattoli, M. Palmery, V. Cuomo, D. Piomelli, *Nat. Med.* **2002**, *9*, 76–81.
[16] S. Y. Sit, C. Conway, R. Bertekap, K. Xie, C. Bourin, K. Burris, H. Deng, *Bioorg. Med. Chem. Lett.* **2007**, *17*, 3287–3291.
[17] M. Mileni, J. Garfunkle, C. Ezzili, F. S. Kimball, B. F. Cravatt, R. C. Stevens, D. L. Boger, *J. Med. Chem.* **2010**, *53*, 230–240.
[18] L. Forster, J. Ludwig, M. Kaptur, S. Bovens, A. Schulze Elfringhoff, A. Holtfrerich, M. Lehr, *Bioorg. Med. Chem.* **2010**, *18*, 945–952.

[19] D. S. Johnson, C. Stiff, S. E. Lazerwith, S. R. Kesten, L. K. Fay, M. Morris, D. Beidler, M. B. Liimatta, S. E. Smith, D. T. Dudley, N. Sadagopan, S. N. Bhattachar, S. J. Kesten, T. K. Nomanbhoy, B. F. Cravatt, K. Ahn, *ACS Med. Chem. Lett.* **2011**, *2*, 91–96.

[20] *ClinicalTrials.gov* (www.clinicaltrials.gov): a) Identifier NCT01618656; b) Identifier NCT01665573; c) Identifier NCT02134080.

[21] T. Terwege, H. Dahlhaus, W. Hanekamp, M. Lehr, *Med. Chem. Commun.* **2014**, *5*, 932–936.

[22] G. Dannhardt, M. Lehr, *Arch. Pharm.* **1993**, *326*, 157–162.

[23] F. Bellina, S. Cauteruccio, A. Di Fiore, C. Marchetti, R. Rossi, *Tetrahedron* **2008**, *64*, 6060–6072.

[24] M. Ishihara, H. Togo, *Synlett* **2006**, 227–230.

[25] A. Könnecke, E. Kleinpeter, *Org. Magn. Reson.* **1979**, *12*, 667–672.

[26] G. Ortar, M. G. Cascio, A. S. Moriello, M. Camalli, E. Morera, M. Nalli, V. Di Marzo, *Eur. J. Med. Chem.* **2008**, *43*, 62–72.

[27] L. Forster, A. Schulze Elfringhoff, M. Lehr, *Anal. Bioanal. Chem.* **2009**, *394*, 1679–1685.

[28] A. Holtfrerich, W. Hanekamp, M. Lehr, *Eur. J. Med. Chem.* **2013**, *63*, 64–75.

[29] T. Ishii, T. Sugane, J. Maeda, F. Narazaki, A. Kakefuda, K. Sato, T. Takahashi, T. Kanayama, C. Saitoh, J. Suzuki, C. Kanai (Astellas Pharma Inc.), Int. PCT Pub. No. WO 2006088075 A1, **2006**.

[30] J. P. Alexander, B. F. Cravatt, *Chem. Biol.* **2005**, *12*, 1179–1187.

[31] J. Z. Patel, S. Ahenkorah, M. Vaara, M. Staszewski, Y. Adams, T. Laitinen, D. Navia-Paldanius, T. Parkkari, J. R. Savinainen, K. Walczyński, J. T. Laitinen, T. J. Nevalainen, *Bioorg. Med. Chem. Lett.* **2015**, *25*, 1436–1442.

[32] A. Holtfrerich, T. Makharadze, M. Lehr, *Anal. Biochem.* **2010**, *399*, 218–224.

[33] W. Hanekamp, M. Lehr, *J. Chromatogr. B* **2012**, *900*, 79–84.

[34] F. Vacondio, C. Silva, A. Lodola, C. Carmi, S. Rivara, A. Duranti, A. Tontini, S. Sanchini, J. R. Clapper, D. Piomelli, G. Tarzia, M. Mor, *Eur. J. Med. Chem.* **2011**, *46*, 4466–4473.

[35] F. Vacondio, C. Silva, M. Mor, B. Testa, *Drug Metab. Rev.* **2010**, *42*, 551–589.

[36] G. Colombano, C. Albani, G. Ottonello, A. Ribeiro, R. Scarpelli, G. Tarozzo, J. Daglian, K. M. Jung, D. Piomelli, T. Bandiera, *ChemMedChem* **2015**, *10*, 380–395.

[37] G. Mata, V. E. do Rosário, J. Iley, L. Constantino, R. Moreira, *Bioorg. Med. Chem.* **2012**, *20*, 886–992.

[38] F. Vacondio, C. Silva, A. Lodola, A. Fioni, S. Rivara, A. Duranti, A. Tontini, S. Sanchini, J. R. Clapper, D. Piomelli, M. Mor, G. Tarzia, *ChemMedChem* **2009**, *4*, 1495–1504.

[39] B. Li, M. Sedlacek, I. Manoharan, R. Boopathy, E. G. Duysen, P. Masson, O. Lockridge, *Biochem. Pharmacol.* **2005**, *70*, 1673–1684.

[40] F. G. Bahar, K. Ohura, T. Ogihara, T. Imai, *J. Pharm. Sci.* **2012**, *101*, 3979–3988.

[41] E. V. Rudakova, N. P. Boltneva, G. F. Makhaeva, *Bull. Exp. Biol. Med.* **2011**, *152*, 73–75.

[42] L. M. Berry, L. Wollenberg, Z. Zhao, *Drug Metab. Lett.* **2009**, *3*, 70–77.

[43] Y. Sakurai, S. F. Ma, H. Watanabe, N. Yamaotsu, S. Hirono, Y. Kurono, U. Kragh-Hansen, M. Otagiri, *Pharm. Res.* **2004**, *21*, 285–292.

[44] B. Brus, U. Košak, S. Turk, A. Pišlar, N. Coquelle, J. Kos, J. Stojan, J. P. Colletier, S. Gobec, *J. Med. Chem.* **2014**, *57*, 8167–8179.

[45] T. Hioki, T. Fukami, M. Nakajima, T. Yokoi, *Drug Metab. Dispos.* **2011**, *39*, 1345–1352.

[46] T. Ishizuka, I. Fujimori, M. Kato, C. Noji-Sakikawa, M. Saito, Y. Yoshigae, K. Kubota, A. Kurihara, T. Izumi, T. Ikeda, O. Okazaki, *J. Biol. Chem.* **2010**, *285*, 11892–11902.

[47] S. Thierbach, K. Büldt-Karentzopoulo, A. Dreiling, U. Hennecke, S. König, S. Fetzner, *ChemBioChem* **2012**, *13*, 1125–1127.

[48] M. Lehr, T. Terwege, German Pat. Appl. DE102012018115 A1, **2014**.

[49] K. Lee, S.-B. Han, E.-M. Yoo, S.-R. Chung, H. Oh, S. Hong, *Synth. Commun.* **2004**, *34*, 1775–1782.

[50] *Molecular Operating Environment (MOE)*, 2013.08; Chemical Computing Group Inc., 1010 Sherbooke Street West, Suite #910, Montréal, QC, H3A 2R7 (Canada), **2015**.

[51] M. L. Verdonk, J. C. Cole, M. J. Hartshorn, C. W. Murray, R. D. Taylor, *Proteins Struct. Funct. Bioinf.* **2003**, *52*, 609–623.

[52] E. F. Pettersen, T. D. Goddard, C. C. Huang, G. S. Couch, D. M. Greenblatt, E. C. Meng, T. E. Ferrin, *J. Comput. Chem.* **2004**, *25*, 1605–1612.